Turkish Journal of Chemistry

http://journals.tubitak.gov.tr/chem/

Research Article

Turk J Chem
(2015) 39: 194 – 205

doi:10.3906/kim-1401-59

Synthesis of methyl 4-(9H-carbazole-9-carbanothioylthio) benzoate: electropolymerization and impedimetric study

Murat ATEŞ[1,*], **Nesimi ULUDAĞ**[1], **Fatih ARICAN**[1], **Tolga KARAZEHİR**[1,2]

[1]Department of Chemistry, Faculty of Arts and Sciences, Namık Kemal University, Değirmenaltı Campus, Tekirdağ, Turkey

[2]Department of Chemistry, Faculty of Arts and Sciences, İstanbul Technical University, Maslak, İstanbul, Turkey

Received: 24.01.2014 • **Accepted:** 03.11.2014 • **Published Online:** 23.01.2015 • **Printed:** 20.02.2015

Abstract: Methyl 4-((9H-(carbazole-9-carbanothioylthio) benzoate (MCzCTB) was chemically synthesized and characterized by FTIR, ^{1}H NMR, and ^{13}C NMR. A novel synthesized monomer was electropolymerized on a glassy carbon electrode (GCE) in various initial molar concentrations of $[MCzCTB]_0 =$ 1, 3, 5, and 10 mM in 0.1 M $NaClO_4/CH_3CN$ and 1 M H_2SO_4. P(MCzCTB)/GCE was characterized by cyclic voltammetry, Fourier transform infrared-attenuated transmittance reflectance, scanning electron microscopy-energy dispersive X-ray, and electrochemical impedance spectroscopy. The capacitive behavior of the modified electrode was obtained by Nyquist, Bode-magnitude, and Bode-phase plots. The highest capacitance at low frequency was obtained as $\sim$53.1 mF cm^{-2} from Nyquist plot and 19.454 Fg^{-1} at a scan rate of 10 mV s^{-1} for $[MCzCTB]_0 = 1.0$ mM. CS_2 and OCH_3 groups are electron-withdrawing and electron-donating groups in the monomer structure. These groups affect the polymerization and capacitive behavior of the polymer. The polymer may be used for supercapacitor and biosensor applications in the future.

Key words: Methyl 4-((9H-(carbazole-9-carbanothioylthio) benzoate, electrochemical impedance spectroscopy, capacitor, electropolymerization, synthesis, SEM images

1. Introduction

Conducting polymers have received considerable attention due to their versatile promising technological applications,[1] such as conductivity, electroactivity, switchable and tunable semiconductivity, solar conversion, and energy storage capabilities.[2,3] Carbazole-based polymers have received much attention in recent years due to their interesting thermal,[4,5] electrical,[6] and photophysical properties.[7]

The synthesized monomer, which includes CS_2 and OCH_3 groups together with carbazole monomer, is electrochemically polymerized on a glassy carbon electrode (GCE) to obtain capacitive polymer films. The functional groups in conjugated polymers were used in many applications, such as capacitance, electrochromic, and biosensors.[8–10]

Electrochemical impedance spectroscopy (EIS) has a well-developed theoretical background and established experimental procedures for obtaining electrochemical information, such as charge transfer resistance, Faradaic capacitance, and electrolyte resistance.[11] EIS has been previously used for carbazole derivative papers in electrolytic media, such as 9-benzyl-9H-carbazole ($C_{LF} = 221.4$ μF cm^{-2}),[12] 9-(4-vinylbenzyl)-9H-

*Correspondence: mates@nku.edu.tr

carbazole (C_{LF} = 564.1 μF cm^{-2}),[13] 5-(3,6-di(thiophene-2-yl)-9*H*-carbazole-9-yl) pentane-1-amine (C_{LF} = 5.07 μF cm^{-2}),[14] 9-tosyl-9*H*-carbazole (C_{LF} = 50.0 mF cm^{-2}),[15] 6-(3,6-di(thiophene-2-yl)-9*H*-carbazole-9-yl)-hexanoic acid (C_{LF}= 5.2 mF cm^{-2}),[16] 2-(3,6-bis(2,3-dihydrothieno[3,4,b][1,4]dioxin-5-yl)-9*H*-carbazole-9-yl) ethyl methacrylate (C_{LF} = 4.10 mF cm^{-2}),[17] and 2-(9*H*-carbazole-9-yl)ethyl methacylate (C_{LF} = 424.1 μF cm^{-2}).[18] This novel polymer has a higher low frequency capacitance value (C_{LF} =$\sim$53.1 mF cm^{-2}) than those previously obtained.

This article describes a novel method for synthesis and characterization of methyl 4-((9H-(carbazole-9-carbanothioylthio) benzoate (MCzCTB) by FTIR, ^{1}H NMR, and ^{13}C NMR spectroscopy. EIS was used to evaluate the capacitive performance of P(MCzCTB)/GCE in different initial monomer concentrations ([MCzCTB]$_0$ = 1, 3, 5, and 10 mM) in 0.1 $NaClO_4/CH_3CN$ and 1 M H_2SO_4 solution. P(MCzCTB)/MWCNT was synthesized in monomer-free solution of 1 M H_2SO_4 at different scan rates by cyclic voltammetry (CV). The aim was to calculate the specific capacitance of nanocomposite material in different initial monomer concentrations of 1, 3, 5, and 10 mM.

2. Results and discussion

2.1. Synthesis of MCzCTB

A suspension of NaOH (30 mmol) in dimethylsulfoxide (150 mmol) was prepared in a beaker. Afterwards, carbazole (29.9 mmol) was added under vigorous stirring for 2 h at room temperature. Carbondisulfide (30 mmol) was added dropwise into this mixture, and the resultant reddish solution was stirred for 4 h at room temperature, followed by slow addition of methyl 4-iodobenzoate (30 mmol) in DMSO. The final mixture was stirred for hours. The resultant reaction mixture was poured into a large amount of water and a yellow solid was obtained by filtration. The crude product was purified by silica gel chromatography and crystallized from diethyl ether. The resultant mass (3.7 g) was obtained in a yield of 58% and at a melting point at 214 °C and molecular weight of 391.48 g/mol, with a retention value of R_f: 0.55 in CH_2Cl_2. The formation mechanism of MCzCTB [19] is given in Figure 1.

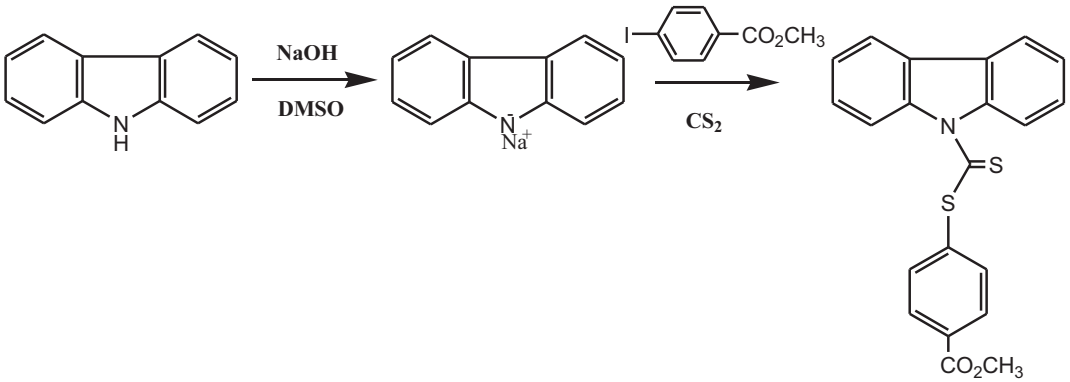

Figure 1. Mechanism of methyl 4-(9*H*-carbazole-9-carbonothioylthio) benzoate.

2.2. Characterization of MCzCTB

The FTIR spectrum of MCzCTB had characteristic peaks given in the following data. FT-IR analysis (potassium bromide): 2975 cm^{-1} (C–H), 1487 cm^{-1} (C=C), 1449 cm^{-1} (aro. C=C).[20] Strong vibrational coupling is

operative in the case of the nitrogen containing thiocarbonyl derivatives and three bands seem to consistently appear in the regions 1395–1570 cm^{-1}, 1260–1420 cm^{-1}, and 940–1140 cm^{-1} due to the mixed vibrations. The N–H peak between 3000 and 3500 cm^{-1} is not observed in the FTIR spectrum. It proves the existence of the CS_2 group in the carbazole structure (Figure 2).

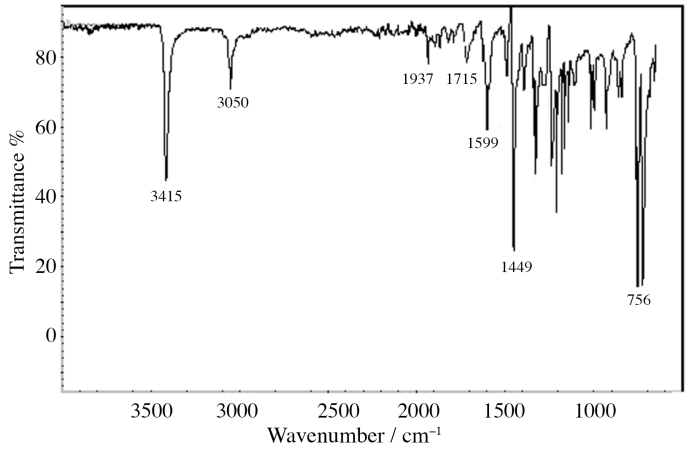

Figure 2. FTIR spectrum of MCzCTB.

The ^{1}H NMR spectrum of MCzCTB had characteristic peaks given in the following data. ^{1}H NMR ((deuteriochloroform): δ 8.10–7.21 (m, aromatic protons, δ 7.21–7.25 (m, aromatic CH), 7.39–8.10 (m, aromatic CH), 4.35 (s, O–CH_3). ^{1}H NMR (deuteriochloroform) spectrum of Cz: δ 7.21–7.25 (m, 4H, aromatic CH), 7.39–7.51 (m, 4H, aromatic CH), 8.09 (s, 1H, NH). There is an important peak difference between carbazole and MCzCTB to prove a novel functional carbazole derivative.

The ^{13}C NMR spectrum of MCzCTB had the following characteristic peaks. ^{13}C NMR (deuteriochloroform): δ 195.6 (C=S), 166.14 (C=O), 140.10, 139.46, 137.66, 136.18, 131.24, 130.12, 131.0, 129.95, 126.9, 125.81, 124.3, 125.12, 123.33, 120.31, 119.41, 115.64, 110.56, 100.54, and 61.24.

Analytically calculated for $C_{21}H_{15}NO_2S_2$ (377.48 g/mol): C (66.82); H (4.01); N (3.71). Found: C (66.85); H (4.97); N (3.74).

2.3. Electropolymerization of MCzCTB

CVs of MCzCTB electrochemically deposited on a GCE in 0.1 M $NaClO_4$/acetonitrile (CH_3CN) at different initial monomer concentrations (1, 3, 5, and 10 mM) are given in Figures 3a–3d. The anodic and cathodic peak potentials were affected by the change in the initial monomer concentrations. During the first anodic scan an irreversible anodic peak at $\sim$1.3 V is observed, attributed to the radical cation formation. The two new peaks observed in the second scan (quasi-reversible peaks) correspond to the oxidation/reduction of short chain oligomers. After the third scan, the formation of the polymer film was obtained on the electrode surface. Thus, the lowest anodic and cathodic peak potential difference (ΔE) was obtained in the initial monomer concentration of $[MCzCTB]_0$ = 5 mM (ΔE = 0.17 V). The other anodic and cathodic peak potential differences (ΔE) were obtained in the following: ΔE = 0.30 V for $[MCzCTB]_0$ = 1 mM, ΔE = 0.43 V for $[MCzCTB]_0$ = 3 mM, and ΔE = 0.24 V for $[MCzCTB]_0$ = 10 mM. The total charges obtained from the electrogrowth process increase by increasing the initial monomer concentrations from 1 mM (Q = 5.90 mC) to 10 mM (Q = 43.28 mC). The

anodic peak potentials appearing at Ep_a =∼1.3 V for $[MCzCTB]_0$ = 1 mM, Ep_a =∼1.39 V for $[MCzCTB]_0$ = 3 mM, Ep_a =∼1.35 V for $[MCzCTB]_0$ = 5 mM, and Ep_a =∼1.46 V for $[MCzCTB]_0$ = 10 mM are attributed to the oxidation peaks of MCzCTB after completion of the electrogrowth process. According to Chen et al., at the oxidation peak potentials, the first radical cations are formed, and two cations are combined to form a dication arising from the head to tail addition of monomer units.[21] The dications were added together to form the oligomeric structure and then to form a random polymer. The cathodic peak potentials appeared at Ep_c =∼1.0 V for $[MCzCTB]_0$ = 1 mM, Ep_c =∼0.96 V for $[MCzCTB]_0$ = 3 mM, Ep_c =∼1.06 V for $[MCzCTB]_0$ = 5 mM, and Ep_c =∼1.03 V for $[MCzCTB]_0$ = 10 mM. By adding the monomer concentration, the anodic and cathodic peaks of the polymer shift to higher values due to the amounts of monomer. Larger amounts of radical cations increase the oligomeric forms. Therefore, the oxidation and reduction potentials shift to higher values.

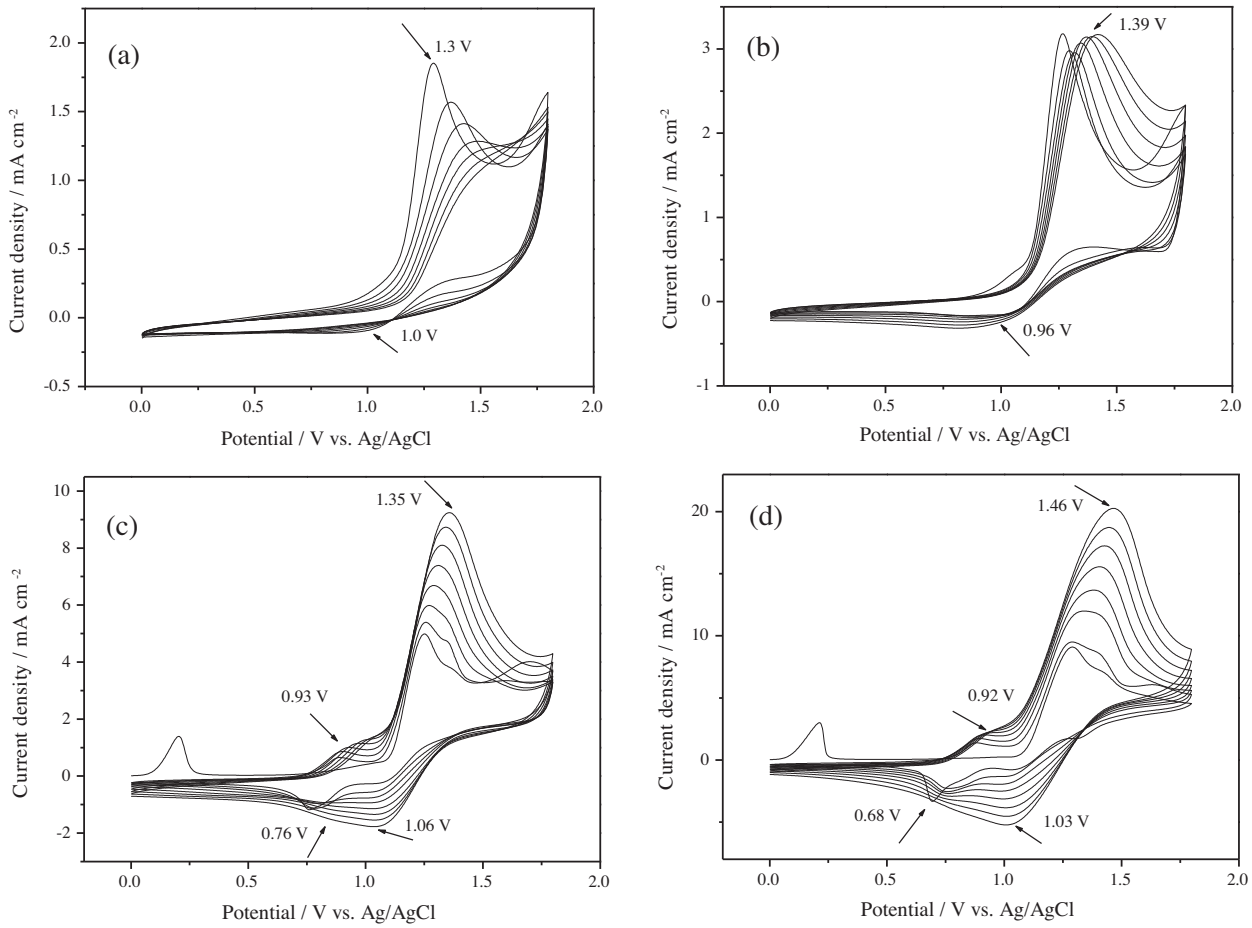

Figure 3. Cyclic voltammetry of MCzCTB was performed on a glassy carbon electrode (GCE) in various initial monomer concentrations in 0.1 M $NaClO_4/CH_3CN$, **a)** $[MCzCTB]_0$ = 1 mM (Q = 5.90 mC), **b)** $[MCzCTB]_0$ = 3 mM (Q = 9.86 mC), **c)** $[MCzCTB]_0$ = 5 mM (Q = 20.14 mC), **d)** $[MCzCTB]_0$ = 10 mM (Q = 43.28 mC). 8 cycles, scan rate: 100 mV s^{-1}. Potential range: 0.0 V–1.8 V.

CVs of MCzCTB also electrochemically deposited on a GCE in 1 M H_2SO_4 solution at different initial monomer concentrations (1, 3, 5, and 10 mM) are given in Figures 4a–4d.

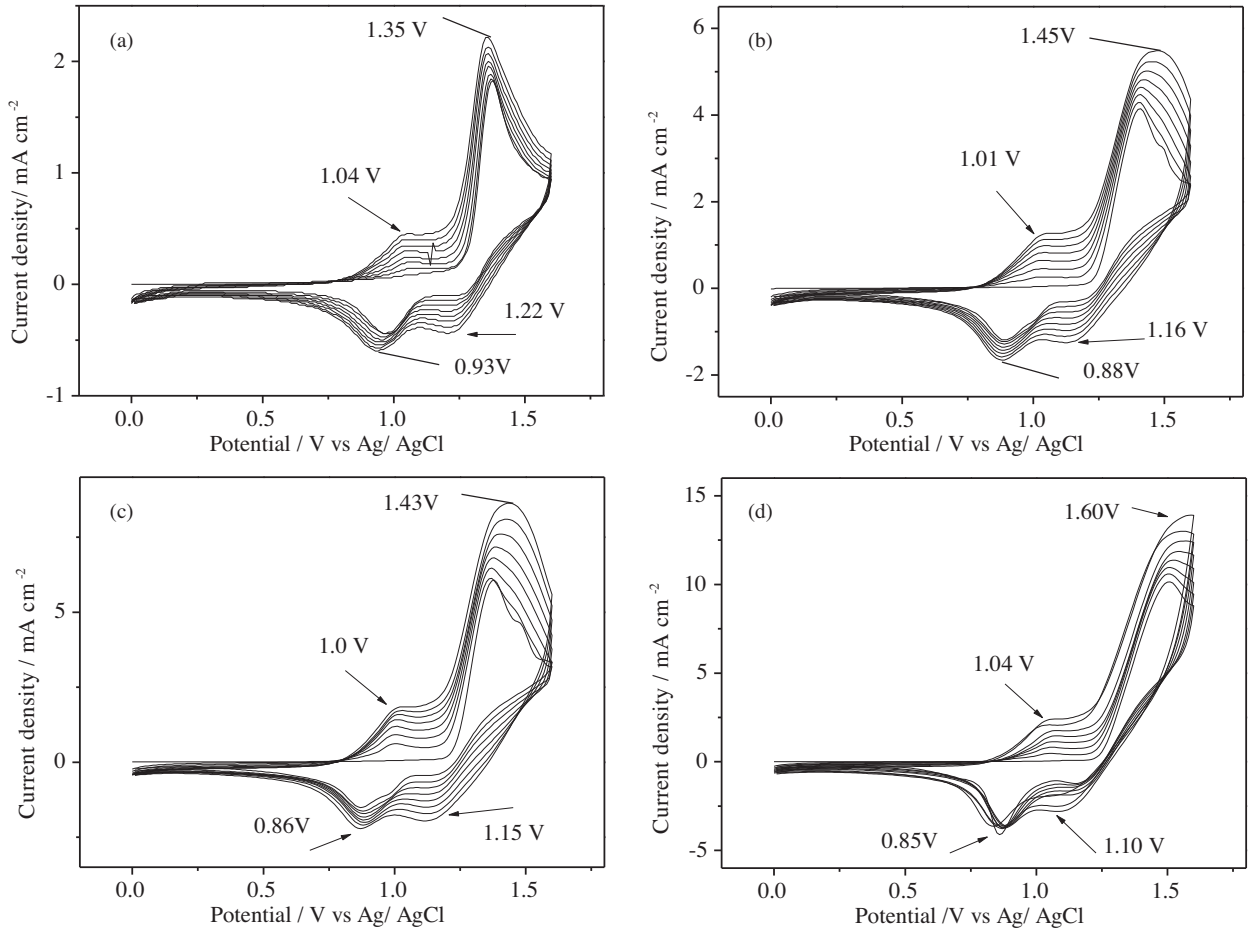

Figure 4. Cyclic voltammetry of MCzCTB was performed on a glassy carbon electrode (GCE) in various initial monomer concentrations in 1 M H_2SO_4 solution, **a)** $[MCzCTB]_0$ = 1 mM, **b)** $[MCzCTB]_0$ = 3 mM, **c)** $[MCzCTB]_0$ = 5 mM, **d)** $[MCzCTB]_0$ = 10 mM, 8 cycle, scan rate: 100 mV s^{-1}. Potential range: 0.0 V–1.6 V.

The P(MCzCTB)/GCE was examined within the applied voltage range of 0.0 to 0.6 V for $[MCzCTB]_0$ = 1.0 mM and 0.0 to 0.4 V for $[MCzCTB]_0$ = 3.0, 5.0 and 10.0 mM at 10, 20, 30, 40, 50, 60, 70, 80, 90, and 100 mV s^{-1} scan rates. The negative and positive current region in the CV curves indicates cathodic reduction and anodic oxidation, respectively. The rectangular shape of the CV curves signifies the redox behavior (Figure 5).

2.4. FTIR-ATR measurements

P(MCzCTB)/carbon fiber microelectrode (CFME) was analyzed by FTIR-ATR. Figure 6 shows the corresponding spectra between 650 and 4000 cm^{-1}. There are sharp peaks of the monomer structure evident in the FTIR measurement. However, there are broad peaks for the polymer structure. Some peaks were also obtained for the monomer at 3415 cm^{-1} (=C–H), 3050 cm^{-1} (aromatic C–H)), 1937 (C–N), 1715 (C=O), 1599 (C=C), 1449 (aromatic C=C), and 756 cm^{-1} (C–S). However, the FTIR spectrum of the polymer peaks at 2345 cm^{-1}, 2113 cm^{-1}, 1739 cm^{-1} (C=O), and 1100 cm^{-1}. The peak at around 1100 cm^{-1} is attributed to the dopant anion ClO_4^- from $NaClO_4$.[22–24] The specific peak of C=S at around 756 cm^{-1} was absent in the polymer structure. These are strong evidence for polymer formation.

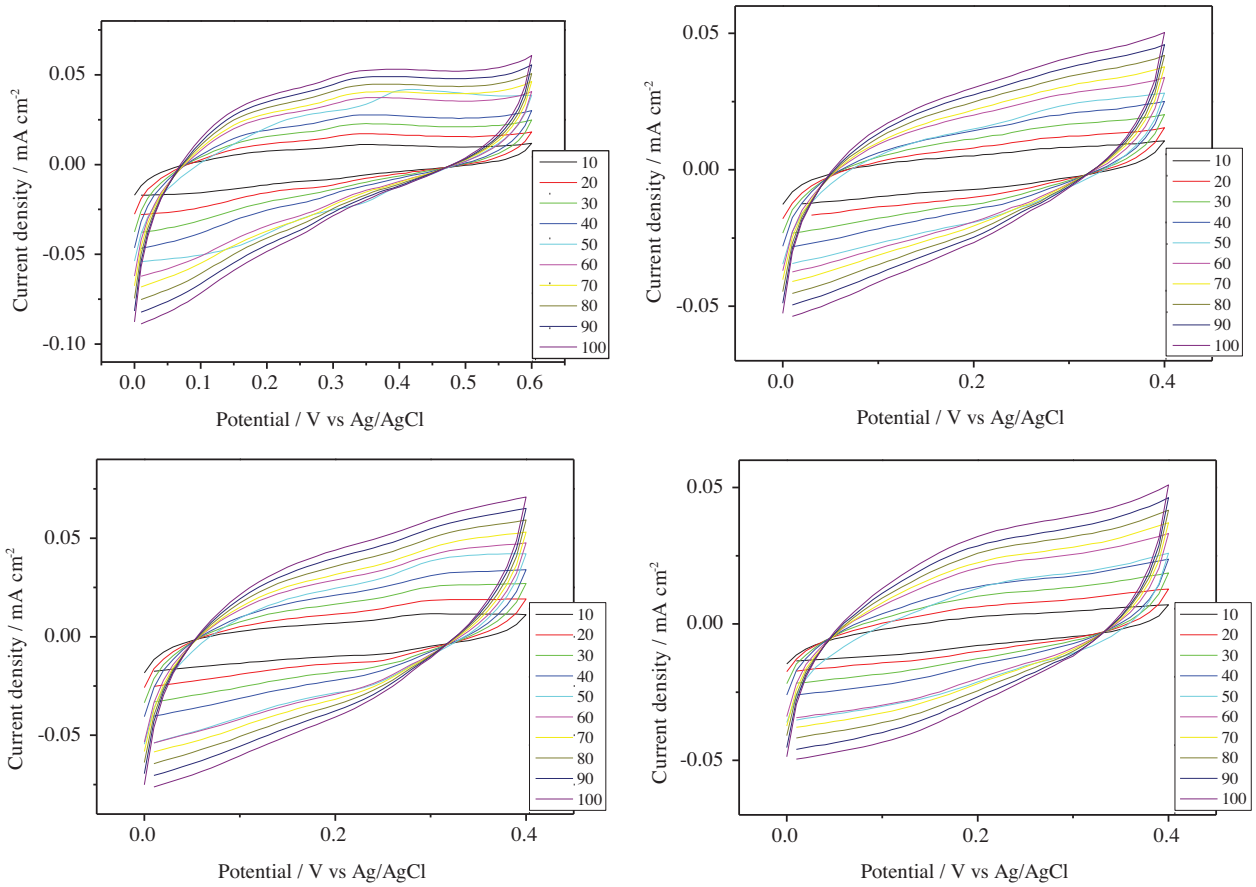

Figure 5. Cyclic voltammetry of MCzCTB was performed in monomer-free solution on a glassy carbon electrode (GCE) in various initial monomer concentrations in 1 M H_2SO_4 solution, **a)** $[MCzCTB]_0$ = 1 mM. Potential range: 0.0 V–0.6 V, **b)** $[MCzCTB]_0$ = 3 mM. Potential range: 0.0 V–0.4 V, **c)** $[MCzCTB]_0$ = 5 mM. Potential range: 0.0 V–0.4 V, **d)** $[MCzCTB]_0$ = 10 mM. Potential range: 0.0 V–0.4 V. Polymerization was performed by 8 cycles, scan rate: 10 mV s^{-1}, scan rates were taken in monomer-free solution as 10, 20, 30, 40, 50, 60, 70, 80, 90, and 100 mV s^{-1}.

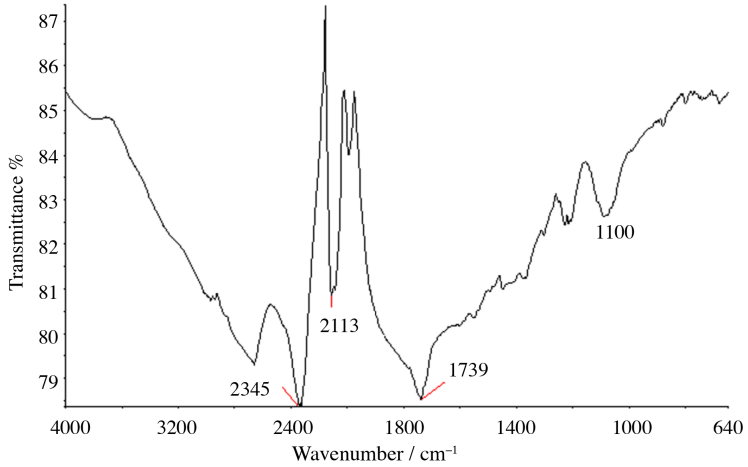

Figure 6. FTIR-ATR spectrum of P(MCzCTB)/CFME, 30 cycles, 0.1 M $NaClO_4/CH_3CN$.

2.5. SEM-EDX measurements

The morphology of the electrocoated P(MCzCTB) was investigated on a single carbon fiber microelectrode (CFME) at different initial monomer concentrations ($[MCzCTB]_0$ = 1, 3, 5, and 10 mM) by scanning electron microscopy (SEM) for samples obtained by cyclic voltammetry, as shown in Figures 7a–7d. In previous studies, polycarbazole obtained electrochemically in 0.1 M $NaClO_4/CH_3CN$ showed a cauliflower-like structure, and a rough surface structure[25] according to SEM and AFM analysis. In our newly synthesized polymer structure, only agglomerates form on the CFMEs in the initial monomer concentration of $[MCzCTB]_0$ = 5 and 10 mM, as shown in Figures 7c and 7d.

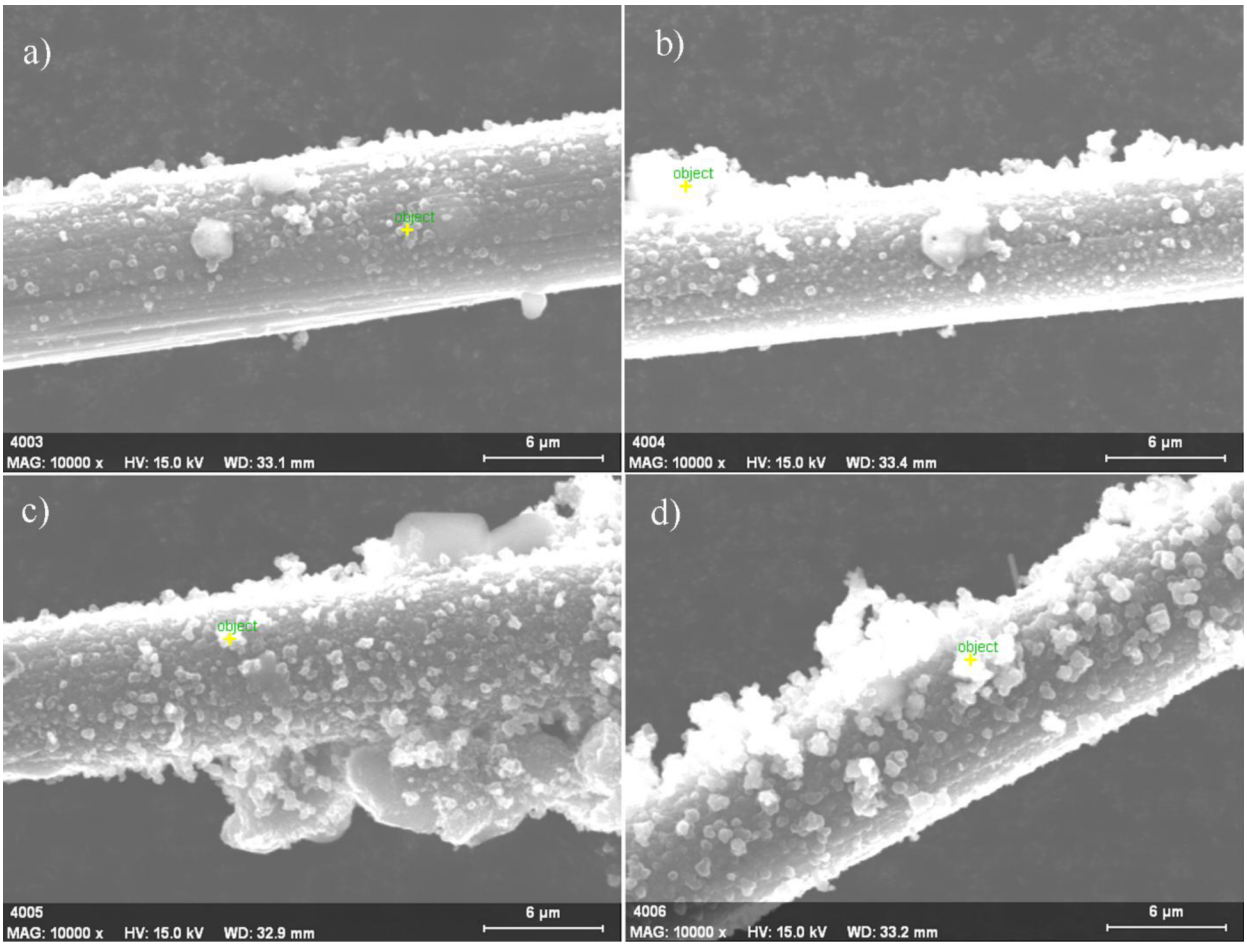

Figure 7. SEM analysis of **a)** $[MCzCTB]_0$ = 1 mM, **b)** $[MCzCTB]_0$ = 3 mM, **c)** $[MCzCTB]_0$ = 5 mM, **d)** $[MCzCTB]_0$ = 10 mM on a single CFME in 0.1 M $NaClO_4/CH_3CN$. Potential range: 0.0–1.8 V, 30 cycles.

Average values of EDX point analysis show the characteristic elements: carbon (~54.13%), oxygen (~21.87%), sodium (~0.55%), chlorine (~0.51%), nitrogen (~17.58%), and sulfur (~5.39%) for $[MCzCTB]_0$ = 10 mM, as shown in Table 1. The average value of EDX point analysis of uncoated CFME was obtained as carbon (98.70%), sodium (1.00%), and chlorine (0.30%). EDX analysis proved the success of the electropolymerization process. The presence of sodium and chlorine in the polymer also proved the successful doping of ClO_4^- anions process into the polymer structure.[26]

Table 1. EDX point analysis of P(MCzCTB)/CFME in 0.1 M $NaClO_4/CH_3CN$. Potential range: 0.0–1.8 V, 30 cycles.

Elements/%	Blank CFME	$[MCzCTB]_0 = 1$ mM	$[MCzCTB]_0 = 3$ mM	$[MCzCTB]_0 = 5$ mM	$[MCzCTB]_0 = 10$ mM
Carbon	98.70	73.59	75.44	55.16	54.13
Oxygen	—	26.04	23.59	23.48	21.87
Sodium	1.00	0.20	0.65	0.64	0.55
Chlorine	0.30	0.17	0.32	0.63	0.51
Nitrogen	—	—	—	20.09	17.58
Sulfur	—	—	—	—	5.39

2.6. Electrochemical impedance spectroscopy study

Electrochemical impedance is a function of alternating current frequency signal. It is generally represented as $Z_{(\omega)} = IZI \times e^{i\theta}$. The film is considered a porous medium.[27,28] Physically, it represents a porous membrane that includes a matrix formed by the conducting polymer with the pores filled with an electrolyte.[29] The low frequency capacitance (C_{LF}) values with different initial monomer concentrations ($[MCzCTB]_0$ = 1, 3, 5 and 10 mM) were obtained from the slope of a plot of the imaginary component (Z_{im}) of the impedance at 10 mHz using the following formula: $C_{LF} = -1/2 \times \pi \times f \times Z_{im}$.[30] The imaginary part of the impedance with a sharp increase in a vertical line means more capacitive behavior of the polymer film. The C_{LF} values were calculated from Nyquist plots as $C_{LF} = 53.1$ mF cm^{-2} for $[MCzCTB]_0 = 1$ mM, $C_{LF} = 26.46$ mF cm^{-2} for $[MCzCTB]_0$ = 3 mM, $C_{LF} = 21.98$ mF cm^{-2} for $[MCzCTB]_0 = 5$ mM, and $C_{LF} = 20.68$ mF cm^{-2} for $[MCzCTB]_0$ = 10 mM, as given in Figure 8. By increasing the initial monomer concentrations, the C_{LF} values decrease. It means that the thin film of P(MCzCTB)/GCE has a higher capacitance (Q = 5.90 mC for $[MCzCTB]_0 = 1$ mM obtained by the electrochemical growth process) than those of the thicker films (Q = 9.86 mC for $[MCzCTB]_0$ = 3 mM, Q = 20.14 mC for $[MCzCTB]_0 = 5$ mM, and Q = 43.28 mC for $[MCzCTB]_0$= 10 mM) (Figure 8).

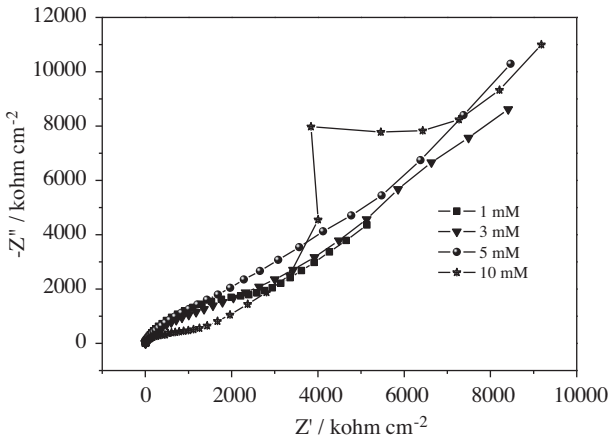

Figure 8. Nyquist plot of P(MCzCTB)/GCE in various initial monomer concentrations (1, 3, 5, and 10 mM). Experimental conditions are given in the following parameters, 8 cycles at a scan rate of 100 mV s^{-1} in 0.1 M $NaClO_4/CH_3CN$.

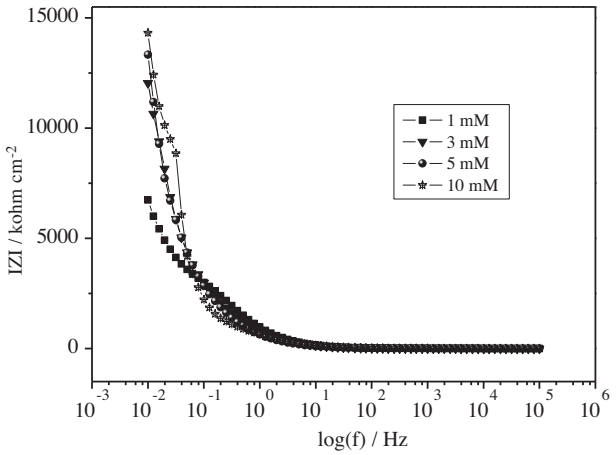

Figure 9. Bode-magnitude plot of P(MCzCTB)/GCE in various initial monomer concentrations (1, 3, 5, and 10 mM). Experimental conditions are given in the following parameters, 8 cycles at a scan rate of 100 mV s^{-1} in 0.1 M $NaClO_4/CH_3CN$.

The Bode-magnitude plot gives [by extrapolating the line to the logZ axis at $\omega = 1$ ($\log\omega = 0$)] the value of double layer capacitance (C_{dl}) from the equation of IZI = $1/C_{dl}$, as given in Figure 9. The C_{dl} values were $\sim$1.39 μF cm^{-2} in 0.1 M $NaClO_4/CH_3CN$ for $[MCzCTB]_0$ = 1, 3, 5, and 10 mM.

If the Bode-phase angle was very close to 90°, more capacitive behavior of the polymer film was obtained in the impedance system. The maximum phase angle was 74° at 82.401 Hz for $[MCzCTB]_0$ = 10 mM. At lower frequencies, such as 14.79 Hz, the phase angles were: $\theta = \sim 61°$ for $[MCzCTB]_0$ = 1 mM, $\theta = \sim 56°$ for $[MCzCTB]_0$ = 3 and 5 mM, and $\theta = \sim 35°$ for $[MCzCTB]_0$ = 10 mM. At low initial concentrations of the monomer, we observed higher phase angles, as shown in Figure 10.

The P(MCzCTB)/GCE modified electrodes with an initial monomer concentration of $[MCzCTB]_0$ = 1 mM had the lowest conductivity according to the admittance plot, as shown in Figure 11. However, they had the highest resistance since the Z' axis exhibited the features of a pure resistor while the Z" exhibited pure capacitive behavior.[31] Additionally, the admittance plot supported the observations deduced from the Nyquist plots.

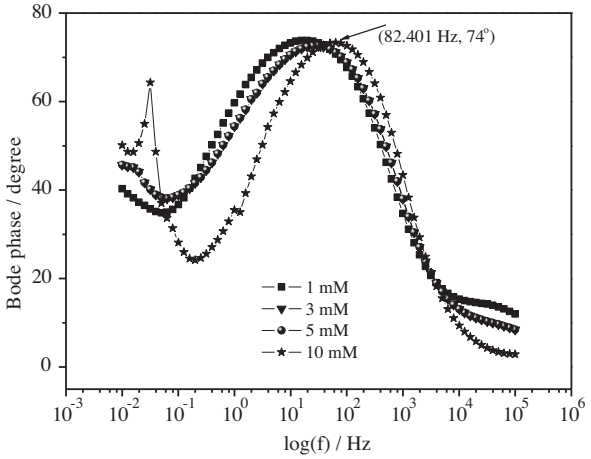

Figure 10. Bode-phase plot of P(MCzCTB)/GCE in various initial monomer concentrations (1, 3, 5, and 10 mM). Experimental conditions are given in the following parameters, 8 cycles at a scan rate of 100 mV s^{-1} in 0.1 M $NaClO_4/CH_3CN$.

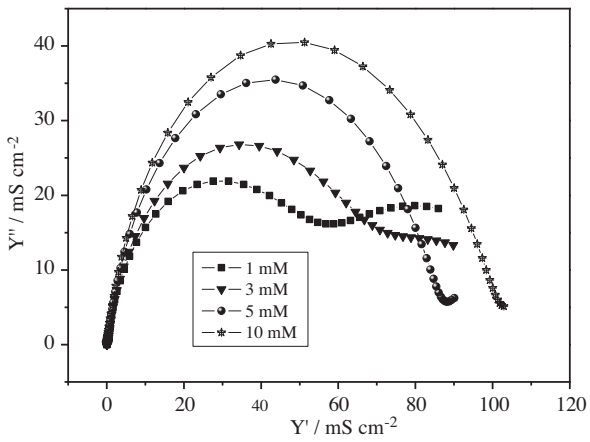

Figure 11. Admittance plot of P(MCzCTB)/GCE in various initial monomer concentrations (1, 3, 5, and 10 mM). Experimental conditions are given in the following parameters, 8 cycles at a scan rate of 100 mV s^{-1} in 0.1 M $NaClO_4/CH_3CN$.

In this study, a novel polymer, MCzCTB, was chemically synthesized and characterized by FTIR, ^{1}H NMR, and ^{13}C NMR spectroscopies. P(MCzCTB)/GCE thin films were obtained at different initial monomer concentrations ($[MCzCTB]_0$ = 1, 3, 5, and 10 mM) by CV. Optimum conditions for evaluating the capacitance of the synthesized polymer via Nyquist, Bode-magnitude, Bode-phase, and admittance plots were established. The highest low frequency capacitance ($C_{LF} = \sim 53.1$ mF cm^{-2}) and phase angle ($\theta = 61°$) and the lowest conductivity were obtained for $[MCzCTB]_0$ = 1 mM. A double layer capacitance C_{dl} of $\sim$1.39 μF cm^{-2} was obtained for $[MCzCTB]_0$ = 1, 3, 5, and 10 mM. The well-defined capacitance analysis of P(MCzCTB)/GCE opens the possibility for supercapacitor and biosensor applications in the future because of the CS_2 and OCH_3 functional groups in the polymer structure. The highest C_{LF} was obtained as 19.454 Fg^{-1} for $[MCzCTB]_0$ = 1 mM at a scan rate of 10 mV s^{-1} as shown in Table 2.

Table 2. Comparative study of different scan rates vs. initial monomer concentrations.

	C_{sp}/Fg^{-1}			
Scan rates/mV s^{-1}	[MCzCTB]$_0$ = 1 mM	[MCzCTB]$_0$ = 3 mM	[MCzCTB]$_0$ = 5 mM	[MCzCTB]$_0$ = 10 mM
10	19.454	6.287	4.164	2.000
20	14.908	3.744	3.210	1.458
30	14.249	3.619	2.903	1.306
40	13.171	3.032	2.694	1.208
50	12.751	2.845	2.784	1.188
60	11.856	2.703	2.452	1.093
70	11.401	2.559	2.434	1.046
80	10.969	2.482	2.241	1.014
90	10.682	2.412	2.182	0.996
100	10.494	2.366	2.132	0.975

The low frequency capacitance after 100 cycles was decreased from 19.51 Fg^{-1} to 10.44 Fg^{-1} (46.49%) for [MCzCTB]$_0$ = 1 mM, compared to 61.6% for [MCzCTB]$_0$ = 3 mM, 49% for [MCzCTB]$_0$ = 5 mM, and 57% for [MCzCTB]$_0$ = 10 mM as shown in Figure 12.

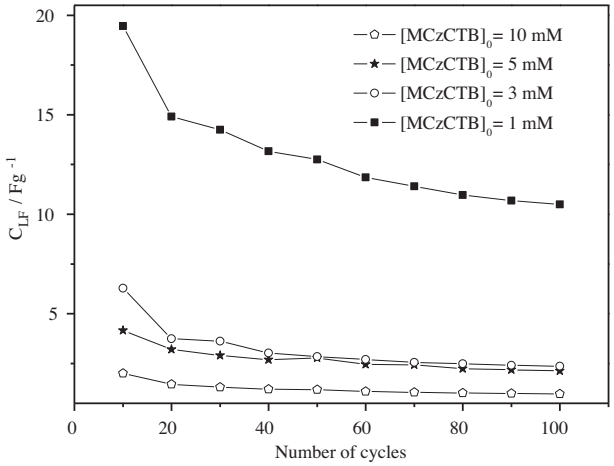

Figure 12. Variation of specific capacitance during 100 cycles in 1 M H_2SO_4 at different initial monomer concentrations of [MCzCTB]$_0$ = 1, 3, 5, and 10 mM.

3. Experimental

3.1. Materials and instrumentation

Carbazole (>95%), carbondisulfide, methyl 4-iodobenzoate, NaOH, and dimethylsulfoxide were purchased from Sigma-Aldrich (Steinheim, Germany) and used without further purification. Silica gel (60 F254) was purchased from Merck (Darmstadt, Germany). Sodium perchlorate (>98%), DMSO, and diethyl ether were obtained from Alfa Aesar (Karsruhe, Germany). Solvents were purified by normal procedures and handled under moisture-free atmosphere. A multi-walled carbon nanotube was obtained with the following properties: average diameter: 8–15 nm; length: ~30 μm, purity: >95%, specific surface area (SSA): 350 m^2/g, (Hayzen Engineering, Ankara, Turkey). All chemicals were high grade reagents and were used as received.

^{1}H NMR spectra were recorded on a Bruker 400 spectrometer operating at 400 MHz. Spectra were registered in $CDCl_3$ using the solvent as an internal standard at 400 MHz for ^{1}H and ^{13}C NMR spectroscopies at room temperature. Chemical shifts are expressed in terms of parts per million (δ) and the coupling constants are given in Hz. Melting points were determined in a capillary tube on Electro thermal IA 9000 apparatus and were uncorrected. Reactions were monitored by thin layer chromatography (silica gel 60 F254). Purification of solvents was performed according to standard methods. CV was performed using PARSTAT 2273 (software: Powersuit and Faraday cage: BASI Cell Stand C3) in a three-electrode configuration, employing a GCE (area: 0.07 cm^2) as the working electrode, platinum wire as the counter electrode, and Ag/AgCl as the reference electrode. A modified carbon fiber microelectrode (CFME) was characterized by Fourier transform infrared - attenuated transmittance reflectance (FTIR-ATR) spectroscopy (PerkinElmer, Spectrum One B, with a universal ATR attachment with a diamond and ZnSe crystal). Morphological investigations were performed with SEM and energy dispersive X-ray analysis (EDX) using a Carl Zeiss Leo 1430 VP.

EIS measurements were performed at different initial monomer concentrations (1, 3, 5 and 10 mM) in 0.1 M $NaClO_4$/acetonitrile (CH_3CN). EIS measurements were done in monomer-free electrolyte solutions with a perturbation amplitude of 10 mV over a frequency range of 0.01 Hz to 100 kHz with a PARSTAT 2273 model potansiostat/galvanostat. CV measurements were performed in a 1 M H_2SO_4 solution at different scan rates from 10 to 100 mV s^{-1}. The capacitances (C_{LF}) were calculated by the following equation:[32–34]

$$C_{LF} = (I_+ - I_-)/\vartheta \times m$$

The polymer mass was calculated by the following formula:

$$Q_{dep} \times M_{mon}/Z \times F$$

In this formula, F: Faraday formula; Z = 2;[35,36] Q_{dep}: Deposition charge; M_{mon}: Monomer mass.

I_+ and I_- are the maximum currents in the positive and negative voltage scans, respectively; ϑ is the scan rate; m is the mass of the composite materials.

3.2. Preparation of the CFMEs

High strength (HS) carbon fibers C 320.000 (CA) single filaments in roving were used as the working electrodes. All of the electrodes were prepared using a 3-cm-long bundle of the CFME (with average diameter of around 7 μm) attached to a copper wire with Teflon tape. The number of carbon fibers in the bundle was about 10. One centimeter of the CFME was dipped into 0.1 M $NaClO_4/CH_3CN$ and monomer solution to keep the electrode area constant (0.022 cm^2) and the rest of the electrode was covered with Teflon tape. The CFMEs were first cleaned with acetone and then dried with an air-dryer before the experiments.[37]

Acknowledgment

This work supported by the Scientific and Technological Council of Turkey (TÜBİTAK): TBAG-110T791 Project.

References

1. Yu, Y. H.; Jen, C. C.; Huang, H. Y.; Wu, P. C.; Huang, C. C.; Yeh, J. M. *J. Appl. Polym. Sci.* **2004**, *91*, 3438–3446.
2. Laforgue, A.; Robitaille, L. *Synth. Met.* **2008**, *158*, 577–584.

3. Ates, M.; Karazehir, T. *Polym. Plast. Technol. Eng.* **2012**, *51*, 1258–1265.
4. Qian, Y. B.; Cao, F.; Guo, W. P. *Tetrahedron* **2013**, *69*, 4169–4175.
5. Kwon, O.; Jo, J.; Walker, B.; Bazen, G. C.; Seo, J. H. *J. Mater. Chem. A,* **2013**, *1*, 7118–7124.
6. Haldar, I.; Biswas, M.; Nayak, A.; Ray, S. S. *J. Nanosci. & Nanotechnol.* **2012**, *12*, 7841–7848.
7. Padalkar, V. S.; Patil, V. S.; Sekar, N. *Chemistry Central Journal* **2011**, *5*, 77–86.
8. Gergely, A.; Inzelt, G. *Electrochem. Commun.* **2001**, *3*, 753–757.
9. MacDiarmid, A. G. *Rev. Mod. Phys.* **2001**, *73*, 701–712.
10. Roncali, J. *J. Mater. Chem.* **1999**, *9*, 1875–1893.
11. Ates, M.; Sarac, A. S. *Prog. Org. Coat.* **2009**, *65*, 281–287.
12. Ates, M.; Uludag, N. *Fibers and Polymers* **2011**, *12*, 296–302.
13. Ates, M.; Uludag, N. *Fibers and Polymers* **2010**, *11*, 331–337.
14. Ates, M.; Uludag, N. *Polymer-Plastics Technology and Engineering* **2012**, *51*, 640–646.
15. Ates, M.; Uludag, N. *Fibers and Polymers* **2011**, *12*, 8–14.
16. Ates, M.; Uludag, N. *Designed Monomers and Polymers* **2013**, *16*, 398–406.
17. Ates, M.; Uludag, N.; Karazehir, T.; Arican, F. *J. Electrochem. Soc.* **2013**; *160*, G46–G54.
18. Ates, M.; Uludag, N.; Sarac, A. S. *J. Appl. Polym. Sci.* **2011**, *121*, 3475–3482.
19. Kato, Y.; Conn, M.M.; Rebek, J. *J. Am. Chem. Soc.* **1994**, *116*, 3279–3284.
20. Gutierrez, O. Y.; Zhong, L. S.; Zhu, Y. Z.; Lercher, J. A. *Chemcatchem.* **2013**, *5*, 3249–3259.
21. Chen, W. C.; Wen, T. C.; Gopalan, A. *J. Electrochem. Soc.* **2001**, *148*, E427–E434.
22. Mohan, K. R.; Achari, V. B. S.; Rao, V. V. R. N.; Sharma, A. K. *Polymer Testing* **2011**, *30*, 881–886.
23. Zotti, G.; Zecchin, S.; Schiavan, G.; Seraglia, R.; Berlin, A.; Canavesi, A. *Chem. Mater.* **1994**, *6*, 1742–1748.
24. Sarac, A. S.; Gilsing, H. D.; Gencturk, A.; Schulz, B. *Prog. Org. Coat.* **2007**, *60*, 281–286.
25. Taoudi, H.; Bernede, J. C.; Bonnet, A.; Morsli, M.; Godoy, A. *Thin Solid Films* **1997**, *304*, 48–55.
26. Desbenemonvernay, A.; Lacaze, P. C.; Dubois, J. E. *J. Electroanal. Chem.* **1981**, *12*, 229–241.
27. Rubinstein, I.; Sabatini, E.; Rishpon, J. *J. Electrochem. Soc.* **1987**, *134*, 3079–3085.
28. Paulse, C. D.; Pickup, P. G. *J. Phys. Chem.* **1988**, *92*, 7002–7006.
29. Vorotyntsev, M. A.; Badiali, J. P.; Inzelt, G. *J. Electroanal. Chem.* **1999**, *472*, 7–19.
30. Sarac, A. S.; Ates, M.; Parlak, E. A.; Turcu, E. F. *J. Electrochem. Soc.* **2007**, *154*, D283–D291.
31. Sarac, A. S.; Ates, M.; Kilic, B. *Int. J. Electrochem. Sci.* **2008**, *3*, 777–786.
32. Sahoo, S.; Karthikeyan, G.; Nayak, G. C.; Das, C. K.; *Synth. Met.* **2011**, *161*, 1713–1719.
33. Dhibar, S.; Sahoo, S.; Das, C. K.; Singh, R. *J. Mater. Sci. Mater. Electron.* **2013**, *24*, 576–585.
34. Wang, J.; Xu, Y. L.; Sun, X. F.; Mao, S. C.; Xiao, F. *J. Electrochem. Soc.* **2007**, *154*, C445–C450.
35. Geetha, S.; Trivedi, D. C. *Synth. Met.* **2005**, *155*, 232–239.
36. Aradilla, D.; Estrany, F.; Aleman, C. *J. Phys. Chem. C.* **2011**, 115, 8430–8438.
37. Sarac, A. S.; Sezgin, S.; Turhan, C. M. *Adv. Polym. Technol.* **2009**, *28*, 120–130.